LATTICE BOLTZMANN SIMULATION OF CHLORIDE TRANSPORT IN ALKALI-ACTIVATED SLAG

Zhiyuan Xu (1), Yibing Zuo (2), Guang Ye (1)

(1) Microlab, Section of Materials and Environment, Faculty of Civil Engineering and Geosciences, Delft University of Technology, Delft 2628 CN, the Netherlands

(2) School of Civil Engineering and Mechanics, Huazhong University of Science and Technology, Wuhan, China

Abstract

In this work, a numerical model is proposed to study chloride transport in alkali-activated materials. This model is based on multiple-relaxation-time lattice Boltzmann method, where particle distribution function is introduced to simulate the chloride binding and diffusion. This model takes into account diffusion, homogenous reaction between chloride ions and diffusive solid, and heterogeneous reaction between chloride ions and non-diffusive solid. The accuracy of the model is confirmed by a benchmark simulation of transient reactive transport problem. As a demonstration, this model is then applied to simulate chloride transport in alkali-activated slag paste with varying alkaline activators. The influence of alkali content, silica content, curing age and chloride binding on the chloride transport property is briefly discussed.

Keywords: lattice Boltzmann method, chloride transport, alkali-activated slag, chloride binding

1. INTRODUCTION

Chloride ingress from external sources, e.g., marine environment or de-icing salts, is the dominant cause for the steel rebar corrosion in the reinforced concrete. The steel rebar is protected by a layer of iron oxide formed on its surface, which results from the high alkaline environment provided by the cement paste. However, a sufficient amount of chloride ions penetrated onto the surface of the steel rebar will break down the passive layer and then initiate the rebar corrosion, which in the end may lead to the structure failure [1].

Alkali-activated materials (AAMs), synthesized by the reaction between aluminosilicate precursor and alkaline activators, have emerged as promising alternatives with low carbon footprint and comparable compressive strength to Portland cement [2]. Although the growing technology of AAMs is drawing a lot of attention in the engineering and research fields [3], only a few experimental studies focused on the chloride transport [3-5] and no numerical study has been carried out in this aspect.

The simulation of chloride transport is significantly dependent on the microstructure of cementitious material. Recently, Zuo developed a numerical framework to simulate the hydration and microstructure formation of alkali-activated materials, called GeoMicro3D [6]. It is composed of four modules, parking of precursors, dissolution of precursors, formation of reaction products, nucleation and growth. All the modules were validated through experimental results, showing the numerical framework can fairly predict the reaction process and microstructure development. Over the last two decades, the lattice Boltzmann method has attracted considerable attention due to its simplicity and accuracy in solving problems with complex boundaries such as fluid flow and convective diffusion in porous media. A detailed introduction and implementation are presented in the next section.

The aim of this study is to present a numerical model to simulate the chloride transport in the alkali-activated materials. The simulation is based on the microstructure generated from GeoMicro3D and lattice Boltzmann method. The numerical model is firstly validated by a benchmark case and then applied to chloride transport in the alkali-activated slag paste.

2. NUMERICAL METHOD

2.1 Lattice Boltzmann method for reactive diffusion

Chloride transport in the cementitious materials is a reactive transport problem. The governing equation for this process can be written as

$$\frac{\partial \phi C}{\partial t} = \nabla \cdot \left(\phi D_p \nabla C \right) + R_{\text{hom}}, \tag{1}$$

where C is the chloride concentration, ϕ is local voxel porosity, D_p is the local chloride diffusivity and R_{hom} is the homogenous reaction caused by chloride binding. Many studies have used lattice Boltzmann method to solve reactive transport problem [7, 8]. Different from conventional numerical methods such as finite volume method, lattice Boltzmann method solves the governing equation by tracking the evolution of particle distribution function $g_i(\mathbf{x},t)$. The evolution of the $g_i(\mathbf{x},t)$ follows the lattice Boltzmann equation

$$g_i\left(\mathbf{x}+\mathbf{e}_i\delta t, t+\delta t\right) - g_i(\mathbf{x},t) = \Omega_i\left(\mathbf{x},t\right) + Q_i\left(\mathbf{x},t\right), \tag{2}$$

where Ω_i is the collision operator, Q_i is the source term due to homogenous reaction and $\mathbf{e}_i$ is the discrete velocity in ith direction. The obtained particle distribution function g_i will be used to calculate the macroscopic variable, which is $\phi C = \sum_i g_i$ in this reactive transport problem. In three-dimension, a lattice structure of 19 velocity directions (D3Q19) is usually adopted in fluid mechanics. However, it is reported that the velocity directions can be decreased from 19 to 7 (D3Q7) without compromising the numerical accuracy in the pure diffusion process without convective term [9]. Thus the lattice structure of D3Q7 is employed in the present model to avoid unnecessary computation. The discrete velocity $\mathbf{e}_i$ is given as $\mathbf{e}_0 = (0,0,0)$, $\mathbf{e}_{1,2} = (\pm 1,0,0)$, $\mathbf{e}_{3,4} = (0,\pm 1,0)$ and $\mathbf{e}_{5,6} = (0,0,\pm 1)$. There are several different collision operators available in the framework of lattice Boltzmann method. Bhatnagar-Gross-Krook (BGK) operator is probably most frequently used due to its simplicity. However, BGK operator is criticized for the dependence of numerical results on the relaxation parameter [10]. To

eliminate such artificial results, multiple-relaxation-time (MRT) scheme is adopted in the present model, which has been demonstrated more suitable, in terms of accuracy and stability, to study transport problem [10, 11]. The basic process of MRT scheme is to project the particle distribution function g_i onto the seven-dimensional vector space, where each component corresponds to a physically relevant moment of g_i, then relax the moments to equilibrium with different relaxation coefficients and finally project the relaxed moments back onto the original space. Mathematically, the collision operator Ω_i in MRT scheme is given by

$$\Omega_i(\mathbf{x},t) = -\left(\mathbf{M}^{-1}\mathbf{S}\mathbf{M}\right)_{ij}\left[g_j(\mathbf{x},t) - g_j^{(eq)}(\mathbf{x},t)\right], \tag{3}$$

where g_i^{eq} is the equilibrium particle distribution function, **M** is the transformation matrix and **S** is a diagonal relaxation matrix. To recover the governing equation from lattice Boltzmann equation, the equilibrium distribution function is designed as follows [7],

$$g_i^{eq} = w_i C, \tag{4}$$

where ω_i is the weight factor and is defined as,

$$\omega_i = \begin{cases} \dfrac{c_\phi}{2}, & i = 1,\ldots,6 \\ \phi - 3c_\phi, & i = 0 \end{cases}. \tag{5}$$

c_ϕ is an adjustable parameter and is set as $\min(\phi)/3.5$ [7]. To contain certain physically relevant moments, e.g., ion amount, ion flux, the transformation matrix **M** is designed as [12]

$$\mathbf{M} = \begin{bmatrix} 1 & 1 & 1 & 1 & 1 & 1 & 1 \\ 0 & 1 & -1 & 0 & 0 & 0 & 0 \\ 0 & 0 & 0 & 1 & -1 & 0 & 0 \\ 0 & 0 & 0 & 0 & 0 & 1 & -1 \\ 6 & -1 & -1 & -1 & -1 & -1 & -1 \\ 0 & 2 & 2 & -1 & -1 & -1 & -1 \\ 0 & 0 & 0 & 1 & 1 & -1 & -1 \end{bmatrix}. \tag{6}$$

The diagonal relaxation matrix **S** is expressed as $\mathbf{S} = diag\left(s_0, s_1, s_1, s_1, s_2, s_2, s_2\right)$, where s_i is relaxation coefficient for each particle distribution function g_i. The relaxation coefficient s_0 is related to conserved moment ϕC and does not affect the numerical results. In the present model, s_0 is set as 0 for simplicity. Comparing the governing equation and the recovered equation from classic multi-scale Chapman-Enskog analysis, it is found s_1 is related to diffusion coefficient by [7]

$$D_p = \frac{c_\phi}{\phi}\left(\frac{1}{s_1} - \frac{1}{2}\right). \tag{7}$$

s_2 corresponds to the second-order moment and has a significant influence on the accuracy of MRT scheme. It is reported that $s_2 = 2 - s_1$ can eliminate discrete effect of boundary condition,

which can generate a more accurate result [11]. The source term Q_i is introduced to incorporate the homogenous reaction R_{hom}. It is expressed by [13]

$$Q_i = \left[\mathbf{M}^{-1} \left(\mathbf{I} - \frac{\mathbf{S}}{2} \right) \mathbf{M} \right]_{ij} \omega_i R_{\text{hom}}, \tag{8}$$

where **I** is the unit matrix. The macroscopic variable should be recalculated by

$$\phi C = \sum_i g_i \left(\mathbf{x}, t \right) + \frac{1}{2} R_{\text{hom}}, \tag{9}$$

in order to correctly recover the term of homogenous reaction in the governing equation.

2.2 Implementation of numerical method

The microstructure used for chloride transport simulation in this study is generated from GeoMicro3D [6], which is a numerical framework for simulating hydration and microstructure formation of alkali-activated materials. Figure 1 (a) shows the simulated microstructure of alkali-activated slag paste at 28 days. The size of the microstructure is 125 μm ? 125 μm ? 125 μm at the resolution of 1 μm ? 1 μm ? 1 μm per voxel. The microstructure is composed of liquid, unhydrated slag, C-(N-)A-S-H gel and crystalline reaction products. The chloride ions are diffusive in liquid and C-(N-)A-S-H gel and non-diffusive in the rest of the phases. Each voxel can be filled by any combination of these 4 phases. Based on the numerical test, a voxel is considered non-diffusive if the non-diffusive solid volume fraction is larger than 0.688 [6]. Figure 1 (b) shows the distribution of diffusive and non-diffusive area. For diffusive voxel, it can consist of different phases, which generates three cases, shown in Figure 2. The local chloride diffusivity is estimated based on these three cases, by differential effective media theory [14]. In Figure 2 (a), the voxel is composed of one diffusive phase and one non-diffusive phase. The local diffusivity is given as [15]

$$D_p = D_B \phi_B^{5/3}, \tag{10}$$

providing that the non-diffusive inclusions are prolate spheroids. For Figure 2 (b), the diffusive Phase A is considered as spherical inclusions in diffusive Phase B. Thus the local diffusivity can be computed as [15]

$$\left(\frac{D_A - D_p}{D_A - D_B} \right) \left(\frac{D_B}{D_p} \right)^{1/3} = \varphi_B. \tag{11}$$

Three phases, non-diffusive solid and two diffusive phases, form the voxel in Figure 2 (c). The determination of such local diffusivity can combine previous two formulas. Phase A and C can be considered as diffusive Phase AC and the diffusivity is calculated by Eq.(10). Then the local voxel diffusivity is calculated by Eq.(11) considering Phase AC and Phase B as two diffusive phases. The equation is shown as [6]

$$D_{AC} = D_A \left(\frac{\phi_A}{\phi_A + \phi_C} \right)^{5/3}, \quad \left(\frac{D_{AC} - D_p}{D_{AC} - D_B} \right) \left(\frac{D_B}{D_p} \right)^{1/3} = \varphi_B. \tag{12}$$

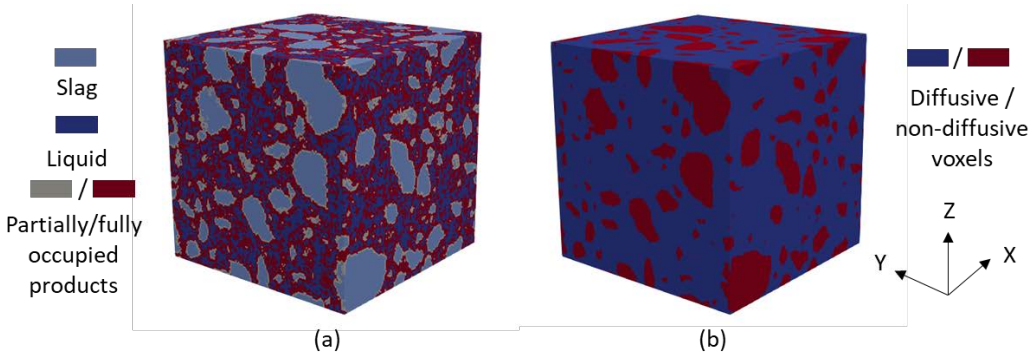

Figure 1: Simulated microstructure of alkali-activated slag paste at 28 days

Since the insufficient knowledge on the transport property of C-(N)-A-S-H gel, the C-(N)-A-S-H gel is considered as the same properties of C-S-H gel. The diffusivity of C-S-H gel is usually obtained indirectly. The reported relative diffusivity of the C-S-H gel ranges from 0.001 [6] to 0.00775 [16]. In the present simulation, the relative diffusivity of C-(N-)A-S-H gel is chosen as 0.002 and the diffusivity of chloride ions in capillary pores is set as 1.5×10^{-10} m^2/s [17]. The porosity of C-(N-)A-S-H is set as 0.3 as the porosity of high-density and low density C-S-H is 0.24 and 0.37 respectively [18]. When the chloride ions transport in the paste, the chloride ions can be bound by reaction products such as C-(N-)A-S-H gel, hydrotalcite (LDH) and strätlingite (AFm). Ke et al. [19] reported that LDH and AFm can bind a great amount of chloride ions and measured their binding capacities. To demonstrate that the present model is able to simulate the chloride transport coupled with chloride binding, the C-(N-)A-S-H gel, LDH and AFm are considered as binding phases and their chloride binding capacities are set as 20 mg/g, 160 mg/g and 130 mg/g respectively [20].

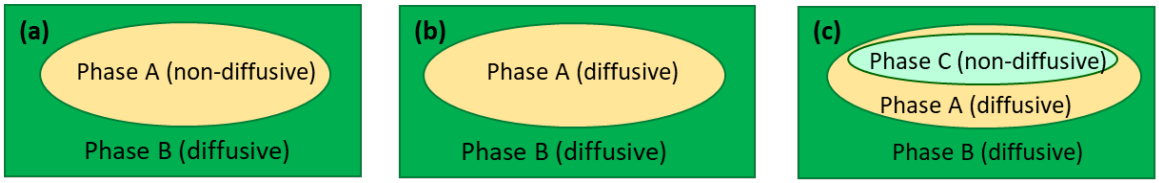

Figure 2: Three cases for local diffusivity

In the simulation, four boundary conditions are implemented, i.e., non-diffusive solid boundary, constant concentration boundary and heterogeneous reactive boundary and periodic boundary. The non-diffusive solid boundary is implemented by half-way bounce-back scheme. The constant concentration is realized by bounce-back scheme at two ends in the x direction, seen in Figure 1. The unknown $g_{\bar{i}}$ entering from outside is determined by exiting g_i and constant boundary concentration C_w, shown as

$$g_{\bar{i}}\left(\mathbf{x},t+\delta t\right)=-g_i^{\dagger}\left(\mathbf{x},t\right)+c_{\phi}C_w. \tag{13}$$

The constant boundary concentration C_w at $x=0$ μm and $x=125$ μm is set as 0.5 mol/L and 0 mol/L respectively, where 0.5 mol/L is chloride concentration in typical seawater. In reality, the chloride binding does not occur instantaneously. It takes at least several hours for reaction

products and chloride ions to reach equilibrium. Kayali et al. [21] showed that 70% binding capacity of hydrotalcite takes place within an hour and the rest binding capacity happens in the next 24 hours. Since the majority of chloride binding occurs in the very beginning, the present numerical model takes the assumption that the binding happens instantaneously, which means chloride ions are removed immediately if the binding capacity of the reaction products is not reached yet. The homogenous reaction R_{hom} is set based on this assumption. For binding phases locating at the non-diffusive solid in contact with the liquid site, i.e., the heterogeneous reactive boundary, the solid site is set as 0 mol/L constant concentration before the binding capacity is reached. The periodic boundary is used in y and z directions, where the exiting particle distribution functions enter from the opposite side.

3. VALIDATION OF NUMERICAL METHOD

To validate the effectiveness and accuracy of the present model, one benchmark case is simulated and the numerical and analytical results are compared. The chosen benchmark case is a transient reactive transport problem in a homogenous porous structure, described by the following equation

$$\frac{\partial \phi C}{\partial t} = \frac{\partial C}{\partial x}\left(\phi D \frac{\partial C}{\partial x}\right) + k_r\left(C_{eq} - C\right), \tag{14}$$

where k_r is the reaction rate constant, C_{eq} is the equilibrium concentration. The porosity ϕ and diffusivity D are constant. This transient problem is also subjected to initial and boundary conditions, which are expressed as

$$C\left(x, t=0\right) = C_{eq}\ ,\ C\left(x=0, t\right) = C_0\,. \tag{15}$$

For this problem, an analytical solution exists and is given by

$$C\left(x,t\right) = C_{eq} - \frac{C_{eq} - C_0}{2}\left(e^{-qx}\operatorname{erfc}\left(\frac{x - \sqrt{b}t/\phi}{2\sqrt{Dt}}\right) + e^{qx}\operatorname{erfc}\left(\frac{x + \sqrt{b}t/\phi}{2\sqrt{Dt}}\right)\right), \tag{16}$$

where b and q can be expressed as $b = 4k_r\phi D$, $q = \sqrt{b}/2\phi D$ respectively.

To simulate this problem, the computational domain is set as $100 \times 20 \times 20\,\text{mm}^3$, where the porosity, diffusivity and reaction rate on each lattice site are constants and set as 0.6, 0.17 mm^2/s and 0.0001 mm/s respectively. The domain initially is filled with solute at equilibrium concentration C_{eq} = 5 mol/L. The left boundary x=0 maintains the constant concentration with C_0 = 10 mol/L and the right boundary is set as open boundary to realize the infinite extension in the right direction. For the above setting, the higher concentration on the boundary will lead to the diffusion of solute downstream and this further results in the reaction of solute due to higher concentration than the equilibrium concentration. The diffusive and reactive process will become steady after a period of time. The present model is used to simulate this reactive transport problem. The comparison of simulated result and analytical result [22] is shown in Figure 3. This figure clearly shows that the present model can accurately predict the transient

concentration distribution in a reactive transport process, which indicates that it can be used in the study of chloride transport.

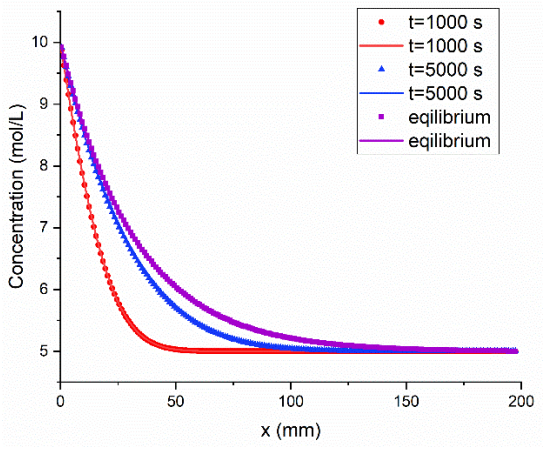

Figure 3: The comparison of solute concentrations between simulated and analytical results. The lines are analytical results and the isolated symbols are simulated results.

4. RESULTS AND DISCUSSIONS

The present model is employed to study chloride transport in the alkali-activated slag paste. Three different pastes are used in this study, i.e., N4S0, N6S0 and N6S5.4. N and S represent Na_2O and SiO_2 and the number behind indicates its weight percentage with respect to the precursor. The water-to-precursor ratio is fixed at 0.4 in all mixtures. The chloride transport simulation is carried out in cubic samples with curing age varying from 12 hours to 28 days. Figure 4 (a) shows the evolution of effective diffusivity as a function of curing age in all three mixtures. Since no effective diffusivity in the alkali-activated slag paste was reported in the literature, the simulated effective diffusivity cannot be quantitatively verified. However, some studies have reported the effective diffusivity in the alkali-activated concrete [3, 4]. As the effective diffusivity in paste should be smaller than that in concrete due to the high porosity of interfacial transitional zone in the concrete, the concrete effective diffusivity can be used to qualitatively verify the simulated results of alkali-activated pastes. The reported effective diffusivity in alkali-activated slag concrete after 28 days is in the range of 10^{-12} to 10^{-11} m^2/s [3, 4]. The simulated effective diffusivity in all three paste mixtures is between 6×10^{-13} and 5×10^{-12} m^2/s, which is reasonable compared to the values reported in the concrete.

As shown in Figure 4 (a), the effective diffusivity decreases as expected with the increase of curing age, due to the ongoing reaction and gradually formed denser microstructure. Figure 4 (a) also shows the influence of sodium content and silica content. Since the average pore size decreases considerably with the increase of sodium content [23], the effective diffusivity is also reported decreasing with more Na_2O content [3]. In the numerical simulation, the effective diffusivity decreases from 5×10^{-12} to 1×10^{-12} m^2/s at 28 days when Na_2O content rises from 4% to 6%, which roughly conforms to the experimental findings. The influence of silica content displayed in the simulation is also consistent with the trend in experiments where increasing silica content at low silica modulus will enhance the resistance to chloride transport [3]. Based on above discussion all the trend shown in the simulation is reasonable and consistent with the experiment.

The present numerical model is also used to study the influence of chloride binding. Figure 4 (b) shows that the chloride concentration is lower when the chloride binding by C-(N-)A-S-H gel, LDH and AFm is considered. This numerically proves that chloride binding can reduce the chloride penetration depth and thus retard the initialization of rebar corrosion.

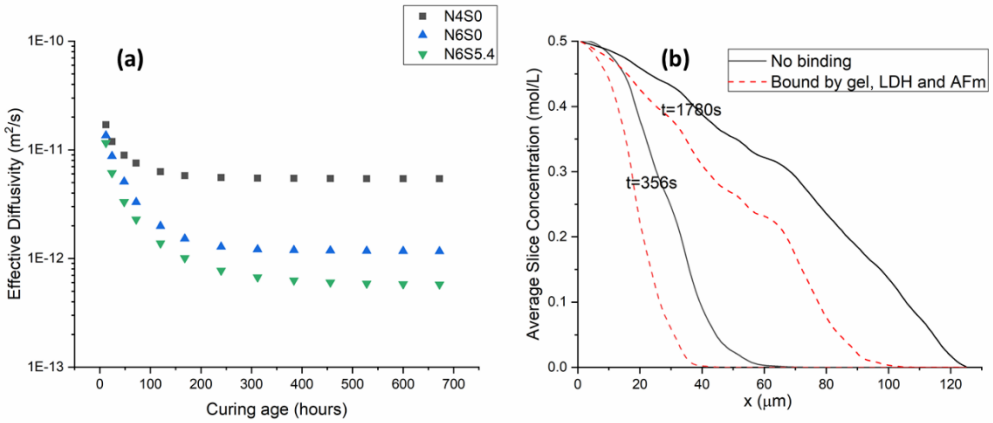

Figure 4: (a) Effective diffusivity in alkali-activated paste with respect to curing age (b) Influence of chloride binding

5. CONCLUSION

In this paper, a lattice Boltzmann method for simulating chloride transport in alkali-activated materials is presented. The numerical model is demonstrated as effective and accurate by simulating a transient reactive transport process. This model then is applied to study chloride transport in a cubic sample of alkali-activated slag paste. The simulated results are compared qualitatively with available experimental results, showing that the current numerical method is a promising numerical tool to predict the chloride transport in alkali-activated materials.

ACKNOWLEDGEMENTS

This work is financially supported by the European Commission through project “PhD Training Network on Durable, Reliable and Sustainable Structures with Alkali-Activated Materials”.

REFERENCES

1. Neville, A. *Chloride Attack of Reinforced-Concrete - an Overview.* Materials and Structures, 1995. **28**(176): p. 63-70.
2. Provis, J.L. and S.A. Bernal *Geopolymers and Related Alkali-Activated Materials.* Annual Review of Materials Research, 2014. **44**: p. 299-327.
3. Ma, Q.M., S.V. Nanukuttan, P.A.M. Basheer, Y. Bai, and C.H. Yang *Chloride transport and the resulting corrosion of steel bars in alkali activated slag concretes.* Materials and Structures, 2016. **49**(9): p. 3663-3677.
4. Dehghan, A., K. Peterson, G. Riehm, and L.H. Bromerchenkel *Application of X-ray microfluorescence for the determination of chloride diffusion coefficients in concrete chloride penetration experiments.* Construction and Building Materials, 2017. **148**: p. 85-95.
5. Ismail, I., S.A. Bernal, J.L. Provis, R.S. Nicolas, D.G. Brice, A.R. Kilcullen, S. Hamdan, and J.S.J. van Deventer *Influence of fly ash on the water and chloride permeability of alkali-activated slag mortars and concretes.* Construction and Building Materials, 2013. **48**: p. 1187-1201.

6. Zuo, Y. and G. Ye *GeoMicro3D: A novel numerical model for simulating the reaction process and microstructure formation of alkali-activated slag.* Cement and Concrete Research, 2021. **141**: p. 106328.
7. Patel, R.A., J. Perko, D. Jacques, G. De Schutter, G. Ye, and K. Van Breugel *A three-dimensional lattice Boltzmann method based reactive transport model to simulate changes in cement paste microstructure due to calcium leaching.* Construction and Building Materials, 2018. **166**: p. 158-170.
8. Kang, Q.J., P.C. Lichtner, and D.X. Zhang *Lattice Boltzmann pore-scale model for multicomponent reactive transport in porous media.* Journal of Geophysical Research-Solid Earth, 2006. **111**(B5).
9. Jeong, N., D.H. Choi, and C.L. Lin *Estimation of thermal and mass diffusivity in a porous medium of complex structure using a lattice Boltzmann method.* International Journal of Heat and Mass Transfer, 2008. **51**(15-16): p. 3913-3923.
10. Chai, Z.H., C.S. Huang, B.C. Shi, and Z.L. Guo *A comparative study on the lattice Boltzmann models for predicting effective diffusivity of porous media.* International Journal of Heat and Mass Transfer, 2016. **98**: p. 687-696.
11. Cui, S.Q., N. Hong, B.C. Shi, and Z.H. Chai *Discrete effect on the halfway bounce-back boundary condition of multiple-relaxation-time lattice Boltzmann model for convection-diffusion equations.* Physical Review E, 2016. **93**(4).
12. Yoshida, H. and M. Nagaoka *Multiple-relaxation-time lattice Boltzmann model for the convection and anisotropic diffusion equation.* Journal of Computational Physics, 2010. **229**(20): p. 7774-7795.
13. Chai, Z.H. and T.S. Zhao *Nonequilibrium scheme for computing the flux of the convection-diffusion equation in the framework of the lattice Boltzmann method.* Physical Review E, 2014. **90**(1).
14. Phan-Thien, N. and D.C. Pham *Differential multiphase models for polydispersed spheroidal inclusions: thermal conductivity and effective viscosity.* International Journal of Engineering Science, 2000. **38**(1): p. 73-88.
15. Patel, R.A. *Lattice Boltzmann Method Based Framework for Simulating Physico-Chemical Processes in Heterogeneous Porous Media and Its Application to Cement Paste*. 2016, Ghent University.
16. Ma, H.Y., D.S. Hou, J. Liu, and Z.J. Li *Estimate the relative electrical conductivity of C-S-H gel from experimental results.* Construction and Building Materials, 2014. **71**: p. 392-396.
17. Zheng, J.J., X.Z. Zhou, and Z.M. Wu *A simple method for predicting the chloride diffusivity of cement paste.* Materials and Structures, 2010. **43**(1-2): p. 99-106.
18. Ulm, F.J., G. Constantinides, and F.H. Heukamp *Is concrete a poromechanics material? - A multiscale investigation of poroelastic properties.* Materials and Structures, 2004. **37**(265): p. 43-58.
19. Ke, X., S.A. Bernal, and J.L. Provis *Uptake of chloride and carbonate by Mg-Al and Ca-Al layered double hydroxides in simulated pore solutions of alkali-activated slag cement.* Cement and Concrete Research, 2017. **100**: p. 1-13.
20. Ke, X. *Improved Durability and Sustainability of Alkali-Activated Slag Cements*. 2017, University of Sheffield: Sheffield.
21. Kayali, O., M.S.H. Khan, and M.S. Ahmed *The role of hydrotalcite in chloride binding and corrosion protection in concretes with ground granulated blast furnace slag.* Cement & Concrete Composites, 2012. **34**(8): p. 936-945.
22. Lichtner, P.C. *Continuum formulation of multicomponent-multiphase reactive transport.* Reactive Transport in Porous Media, 1996. **34**: p. 1-81.
23. Ravikumar, D. and N. Neithalath *Electrically induced chloride ion transport in alkali activated slag concretes and the influence of microstructure.* Cement and Concrete Research, 2013. **47**: p. 31-42.